J. Phys. C: Solid State Phys., **17** (1984) 5833–5850. Printed in Great Britain

The Raman spectra of ice (I_h, II, III, V, VI and IX) as functions of pressure and temperature

B Minceva-Sukarova†, W F Sherman and G R Wilkinson
Department of Physics, King's College London, Strand, London WC2R 2LS, UK

Received 27 February 1984

Abstract. The Raman spectra of various forms of ice I_h, II, III, IX, V and VI of H_2O, D_2O, $H_2{}^{18}O$ and small percentages of HOD in both D_2O and H_2O have been recorded in their true regions of stability. The high-pressure low-temperature Raman cell used for this work is described. The influence of pressure on the OH and OD stretching modes and the lattice vibrational frequencies is discussed. It is estimated that the pressure compresses the O–O bond lengths on average about 5 pm GPa^{-1} in the I_h, II, III and V types of ice. An attempt is made to correlate the available spectroscopic and crystallographic data for the various forms of ice in order to make assignments of the Raman- and infrared-active lattice vibrational spectra.

1. Introduction

Since the pioneer work of Tammann (1900) and Bridgman (1912, 1935, 1937), a vast amount of experimental work has been performed on ice and its high-pressure polymorphs. Much of this work has been done using the recovery technique of quenching the pressurised sample to liquid-nitrogen temperature then releasing the pressure and making observations at atmospheric pressure and low temperature where the sample is metastable. Thanks to this metastable property, the structures of most of the high-pressure polymorphous ices have been determined and some good Raman and infrared spectra have been recorded (Wong and Whalley 1976, Bertie and Bates 1977, Bertie and Francis 1980, 1982).

However, there were several reasons for making this Raman study of the various ice structures in their regions of true stability.

(i) Not all the high-pressure polymorphs can be reclaimed. Ice III for instance, found to be a disordered form of ice IX (Whalley *et al* 1968), can *never* be reclaimed because it always transforms into ice IX on quenching (see figure 1). It can be studied only under pressure.

(ii) The disorder–order transition from ice III to ice IX can be followed spectroscopically under pressure.

(iii) The effects of pressure and temperature on the spectroscopic properties of the ice phases could be followed if the pressure and temperature were varied. In particular,

† Present address: Faculty of Chemistry, Cyril and Methodius University, Arhimedova 5, POB 108, Skopje, Yugoslavia.

0022-3719/84/325833 + 18 $02.25

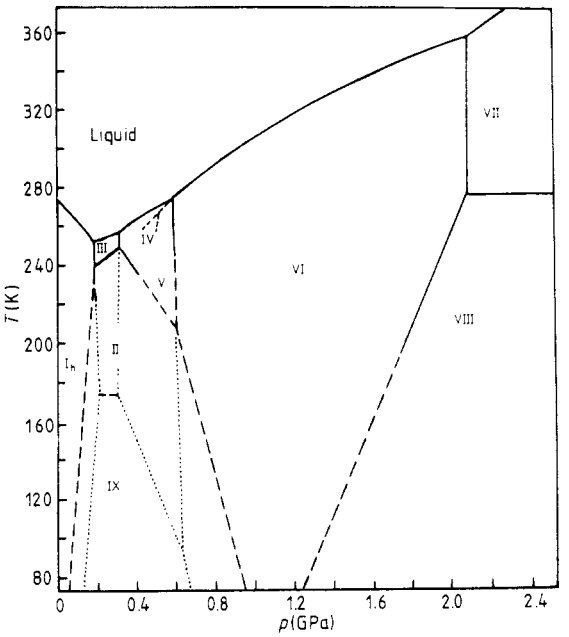

Figure 1. The phase diagram of H_2O (The full and long dashed lines represent directly measured stable and metastable lines respectively, and short dashed and dotted lines represent boundaries that are extrapolated or estimated from the available data).

the effects of pressure and temperature on the Raman spectra of uncoupled HDO vibrations could be studied. This provides information about interatomic distances.

(iv) Understanding of the phase boundaries (figure 1) could be improved as a result of a detailed spectroscopic study of the high-pressure polymorphs in their real regions of stability.

(v) A spectroscopic study of the high-pressure forms of ice in their regions of stability is necessary in order to relate the phases recovered by the quenching technique to the thermodynamically stable forms. (A few *in situ* Raman O–H stretching spectra of the high-pressure forms of ice have been reported (Hawke *et al* 1974, Hirsh and Holzapfel 1980, Abebe and Walrafen 1979) but no lattice mode *in situ* data was available prior to our study.)

Our purpose-built high-pressure low-temperature Raman cell enabled us to record Raman spectra of the high-pressure forms of ice in the range of pressures from 0–0.7 GPa and temperatures from 294 to 140 K. (The cooling system has now been changed to allow studies to be made down to 80 K.)

Soon after the cell was built, (about eight years ago) the Raman spectra of the I_h, II, III and V forms of ice were recorded in the regions of true stability (Kennedy *et al* 1976). This work was restarted recently with the same cell but with a somewhat modified sealing system and using a new Spex Ramalog system (Sukarova 1982, Sukarova *et al* 1982). These changes enabled us to record additionally the spectra of the IX and VI forms of ice. Variable pressure and temperature measurements inside the regions of stability of I_h, II, III, (IX) and V and to some extent VI gave values for $\partial\nu/\partial T$ and $\partial\nu/\partial p$ for most of the strong spectral features.

The present experimental results give information on the nature of the hydrogen bonds within the crystal structure of these forms of ice. A detailed explanation and assignment of every Raman band in each ice form requires a separate study. We give here a general description of our experimental technique and an overview of our results. Detailed discussions on some of the ice forms studied by us will be given elsewhere.

2. Experimental details

2.1. The design of the cell

Figure 2 illustrates the piston-in-cylinder-type high-pressure Raman cell which has been used in the present study. The cell has been designed for generating pressures up to about 1 GPa at temperatures between about 100 and 298 K.

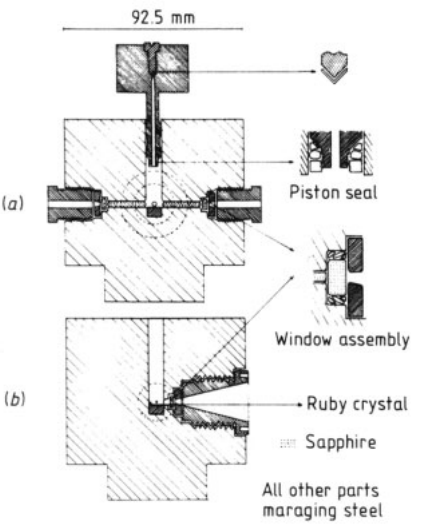

Figure 2. Cross section of the high-pressure cell: (*a*), across the laser window; (*b*), across the Raman collecting window.

The body of the high-pressure vessel was made of 110 maraging steel. It had channels cut near the outside diameter for the cooling fluid (nitrogen gas in the present study) and it was mounted within an outer jacket which served as a vacuum jacket, a safety jacket and the framework for the hydraulic press which forces the piston into the cylinder.

Due to the large volume changes occurring between ice I_h and the high-pressure forms of ice, a piston-type cell was chosen. The design of the high-pressure cell was such that it had holes of approximately 20.5 mm long and 3.2 mm in diameter (figure 2) in both the laser-in and laser-out windows. It was necessary to insert sapphire rods in these holes otherwise the laser light was very badly scattered by the mixture of ice phases produced by the pressure gradients along the holes. The relatively long optical path within the high-pressure cell made it necessary to use a 10 cm focal length lens for focusing the laser beam. This gave a laser beam focus that matched quite well with the F2 optics used for collecting the Raman signal and focusing it onto the entrance slit of the Spex Ramalog system.

The three pressure retaining sapphire windows were sealed with packings of brass, rubber and phosphor–bronze and are schematically represented in the inset in figure 2.

The aperture of the window support plugs has been shaped as suggested by Lavergne and Whalley (1979). In order to reduce the maximum stress in the window material, a radius of about 0.3 mm round the edges of the unsupported area has been made and this was smoothly 'blended-in' to the main flat surface over a radial distance of about 0.5 mm.

An enlarged view of the piston seal is given in the inset in figure 2. An unsupported area wedge-ring seal was used as described by Whalley and Lavergne (1976). In order to ensure that no air bubbles have been formed inside the high-pressure cell, a small channel with a diameter of about 1 mm was drilled along the whole length of the piston which finished with a small screw at the top (figure 2). During loading of the cell the piston was pushed into the water-filled bore. The central piston channel allowed first any trapped air, and then a little water, to be pushed up through the channel. This required another seal at the top of the piston which was made by a hardened steel cone pushing onto an annealed copper gasket.

2.2. *Pressure and temperature controls*

Pressure was generated by a low-pressure piston which was driven by oil from a simple hand pump joined to the cell by a flexible copper coupling. The cooling was achieved by blowing cold nitrogen gas round cooling channels in the outermost parts of the pressure-retained cell. In this way, temperatures down to 140 K could be achieved.

A thermocouple and oil pressure gauge were used for temperature and pressure measurements. The pressure was checked against the frequency shifts of the R_1 ruby luminescence band. A temperature-independent value of $-7.6(2)\ cm^{-1}\,GPa^{-1}$ was used for the pressure shift of the R_1 ruby luminescence line (Piermarini *et al* 1975, Noack and Holzapfel 1977). The temperature dependence of the frequency of the ruby band was carefully measured at zero pressure and the value for the appropriate temperature used as the reference for the pressure measurement. The frequency of the R_1 ruby luminescence line was determined with an accuracy of $\pm 0.1\ cm^{-1}$, which gave an accuracy of the pressure determination in our experiments of about ± 0.02 GPa, which is a value often mentioned in the literature (Sherman 1982).

2.3. *Other experimental details*

The Raman spectra were recorded with a Spex Ramalog 5M System with a Spectra Physics argon ion laser. The 488.0 nm laser line was used throughout this study with the power at the sample being between 0.6 and 1.2 W. In most of the experiments a narrow-band transmission filter was used in the laser path in order to remove the plasma lines.

All frequencies were calibrated against neon emission lines. The frequencies were measured with an accuracy that was typically $\pm 2\ cm^{-1}$ for broad bands but about $\pm 0.5\ cm^{-1}$ for sharper bands. In different parts of this study different resolutions were used in the range between 0.5 and $4.0\ cm^{-1}$, while the scanning speed was varied between 2 and $0.02\ cm^{-1}\,s^{-1}$.

Three types of isotopes, H_2O, D_2O and $H_2{}^{18}O$, and two types of dilute solutions (small percentages of H_2O in D_2O and of D_2O in H_2O) were used in our experiments. All high-pressure H_2O ices were made from redistilled and de-ionised water. Before pouring this into the high-pressure cell, water was boiled for a few minutes in order to drive out gases which are easily accessible and dissolved in water.

The D_2O forms of ice were made from 99.8% D_2O supplied by GOSS Chemicals Ltd. The $H_2{}^{18}O$ ices were made from 99.7% $H_2{}^{18}O$ obtained by courtesy of Dr D Straschewski.

The volume percentage of the dilute solutions of D_2O in H_2O varied from 1 to 5% and the percentage of the dilute solutions of H_2O in D_2O varied from 0.2 to 3%.

3. Results and discussion

An overall impression of the spectra studied here can be obtained from the Raman spectra of ices I_h, II, III, IX, V and VI made from H_2O, from 10–4000 cm^{-1}, which are shown in figure 3.

3.1. General features of the Raman spectra of the uncoupled OD vibrations

The Raman spectra of the $\nu_{OD}(HDO)$ bands are shown in figure 4 and the frequencies are listed in table 1. The shapes of these bands and their frequencies are similar to those

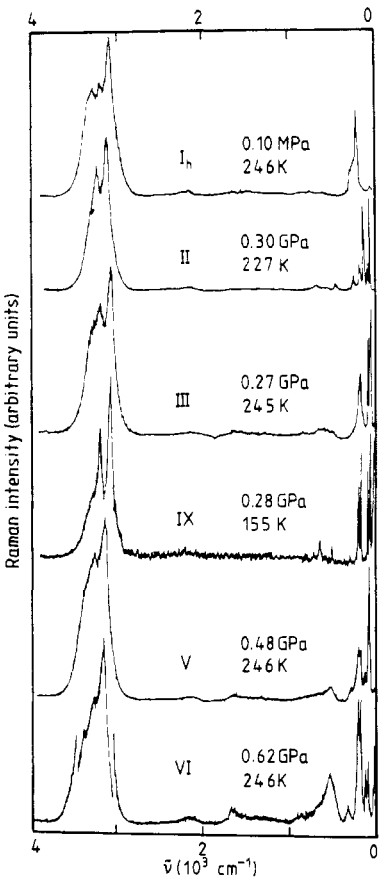

Figure 3. Raman spectra of the I_h, II, III, IX, V and VI forms of ice of H_2O in their regions of stability.

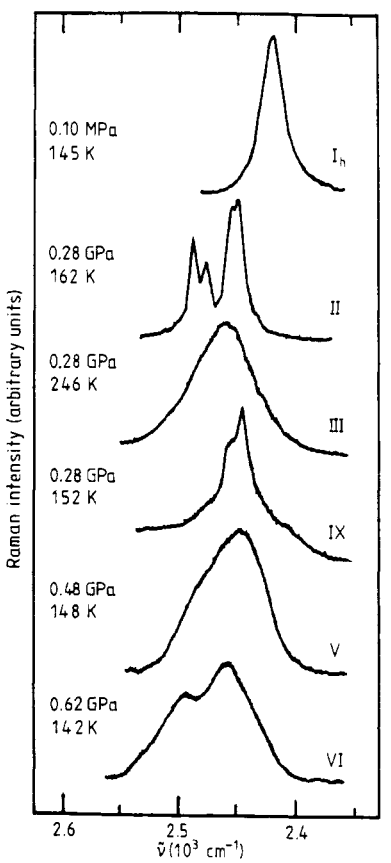

Figure 4. The Raman spectra of the $\nu_{OD(HDO)}$ (2–3% D_2O in H_2O) in the I_h, II, III, IX, V and VI forms of ice at pressures and temperatures as indicated (resolution 2–3 cm^{-1}).

Table 1. Pressure and temperature dependences for the $\nu_{OD(HDO)}$ bands in the different ice phases examined in our experiment.

Ice	p (GPa)	$\nu_{OD(HDO)}$ (cm^{-1})† (Temperature (K))	$\partial\nu/\partial p$ (cm^{-1}/GPa)	$\partial\nu/\partial T$‡ (cm^{-1}/K)
I_h	0.0001	2433 (246 K)	-46.3 ± 1.4	+0.129 (2)
II	0.28	2460 (225 K)	-38.1 ± 7.0	+0.137 (9)
		2488 (224 K)	-41.5 ± 4.0	+0.131 (9)
III	0.28	2456 (246 K)	-40.2 ± 6.8	+0.125 (7)
IX	0.28	2446 (150 K)	—	—
		2457 (150 K)	—	—
V	0.42	2459 (246 K)	-37.0 ± 2.0	+0.150 (10)
VI	0.62	2469 (246 K)	—	+0.143 (7)
		2506 (246 K)	—	+0.159 (9)

† $\Delta\nu = \pm 1\ cm^{-1}$.

‡ The uncertainty in the last decimal place is indicated in brackets.

obtained from the infrared spectra (Bertie and Whalley 1964, Bertie *et al* 1968). The conspicuously lower mean ν_{OD}(HDO) frequency in ice I_h as compared with the mean ν_{OD}(HDO) frequency in each of the other high-pressure forms of ice indicates weaker hydrogen bonds in the other ices.

The existence of proton order and disorder in different ice phases is clearly visible in the shapes and band widths of the ν_{OD}(HDO) bands (figure 4). Thus, the ices I_h, III, V and VI were found to be disordered (at least at temperatures above about 140 K), while the ices II and IX have sharp bands, indicating ordered structures.

The pressure and temperature dependences of the ν_{OD}(HDO) band frequencies for all ices examined in our experiments are listed in table 1. Although the accuracies of the shift rates $\partial\nu/\partial p$ and $\partial\nu/\partial T$ are not impressive these values seem to be the only reported pressure and temperature shifts for the isolated OD frequencies in any of the high-pressure ice forms up to date.

The pressure shift of the OH stretching motion in a dilute solution of D_2O for liquid water in the range from 0–1 GPa and at 298 K was found to be about $-23\ cm^{-1}$/GPa (Walrafen 1973). This value has been used by Whalley (1975) to estimate the extent of compression of the O...O bond length in water. He combined the $\partial\nu/\partial p$ slope obtained by Walrafen with the estimated slope of $\partial\nu_{OD}(HDO)/\partial_{RO-O}$ of 7.7 cm^{-1}/pm and found that the O–O bond contracts by about 3.0 pm/GPa.

Our pressure dependence measurements suggest that the rate at which the O–O bond contracts in I_h, III and V at 246 K and II at 225 K, is -6.0 ± 0.18 pm/GPa, -5.22 ± 0.88 pm/GPa, -4.80 ± 0.26 pm/GPa and -5.17 ± 0.17 pm/GPa respectively. Though the uncertainties are rather large, it seems that the rate of contraction of the O...O bond length with pressure decreases in the order ice I_h, (II, III) and V is real. The value for ice I_h of -6.0 pm/GPa as found in these measurements is not far from the value mentioned by Whalley (1973). Note that temperature- and pressure-dependent data is available for ice I_h (Sivakumar *et al* 1978, Johari and Sivakumar 1978) but not for the high-pressure polymorphs.

3.2. General features of the Raman spectra of the OH and OD vibrations

Raman spectra of the $\nu_{OH}(H_2O)$ and $\nu_{OD}(D_2O)$ bands in the I_h, II, III, IX, V and VI

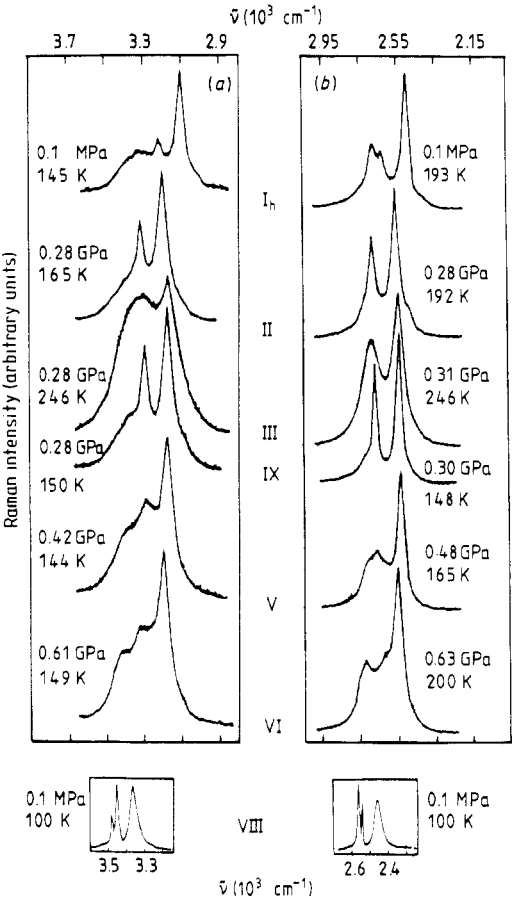

Figure 5. The Raman of (*a*) $\nu_{OH}(H_2O)$ and (*b*) $\nu_{OD}(D_2O)$ spectra of ices I_h, II, III, IX, V, VI and VIII at pressures and temperatures as indicated. (The Raman spectra of ice VIII is from Wong and Whalley (1976).

forms of ice are shown in figure 5. (The Raman spectra of ice VIII of H_2O and D_2O at atmospheric pressure and 100 K have been included in figure 5.)

Although attempts to assign the bands in the O–H stretching region started with the first spectroscopic experiments on ice I_h, there is still only a partial assignment of the Raman bands in this region. The strong Raman band at the lowest O–H stretching frequency is most probably due to ν_1 vibrations of water molecules which are vibrating largely in phase with one another (Whalley 1977). Similar assignments have been proposed for ice VIII (Wong and Whalley 1976) and the II and IX forms of ice (Bertie and Francis 1980).

The precise assignments of two higher-frequency peaks which appear in the O–H stretching region in all the ice phases examined by us are still disputed in the literature.

The pressure and temperature shifts for the strongest Raman band (ν_1) in all ice forms examined in our experiment are given in table 2. A schematic representation of the effect of pressure on the frequencies of the ν_1 OH stretching vibrations in the various ice structures is given in figure 6. Although the pressure-induced shifts for ice in the forms I_h, II, III, IX and V are obtained with rather large uncertainties, (table 2)

Table 2. Frequencies, $\partial\nu/\partial p$ and $\partial\nu/\partial T$ slopes for OH and OD stretching vibrations in pure H_2O and D_2O in various ice phases.

Ice	p (GPa)	$\nu^{\beta}_{OH(H_2O)}$ (cm^{-1})	$\partial\nu_{OH(H_2O)}/\partial p$ (cm^{-1}/GPa)	$\partial\nu_{OH(H_2O)}/\partial T$[b] ($cm^{-1}$/K)	$\nu^{\beta}_{OD(D_2O)}$ (cm^{-1})	$\partial\ \nu_{OD(D_2O)}/\partial p$ (cm^{-1}/GPa)	$\partial\ \nu_{OD(D_2O)}/\partial T$[b] ($cm^{-1}$/K)
I_h	0.0001	3138 (246 K)	−78.0 ± 7.2	+0.38 (3)	2316 (246 K)	—	+0.32 (3)
II	0.28	3208 (225 K)	−79.5 ± 9.5	+0.29 (3)	2364 (225 K)	−42.2 ± 2.1	+0.20 (1)
III	0.28	3175 (246 K)	−82.3 ± 17.5	+0.42 (4)	2344 (246 K)	—	—
IX	0.28	3156 (158 K)	−81.2 ± 8.0	—	2334 (158 K)	−58.0 ± 10.0	—
V	0.42	3193 (248 K)	−92.3 ± 8.1	+0.30 (1)	2365 (248 K)	−55.5 ± 5.1	+0.22 (3)
VI	0.62	3198 (246 K)	−72.0 ± 2.0[e]	+0.12 (3)	2368 (246 K)	—	—
VII[c]	2.53	3255 (289 K)	—	—	—	—	—
VIII[c]	3.12	3277 (256 K)	—	—	—	—	—
VIII[d]	0.0001	3358.8 (100 K)	—	—	2462.7 (100 K)	—	—

[a] $\Delta\nu = \pm 2\ cm^{-1}$, except for ice VII[c] and ice VIII[c] ($\Delta\nu = \pm 8\ cm^{-1}$) and ice VIII[d] ($\Delta\nu = \pm 0.1\ cm^{-1}$).
[b] The uncertainty in the last place is in brackets.
[c] Hirsh and Holzapfel (1981).
[d] Wong and Whalley (1976).
[e] Abebe and Walrafen (1979).

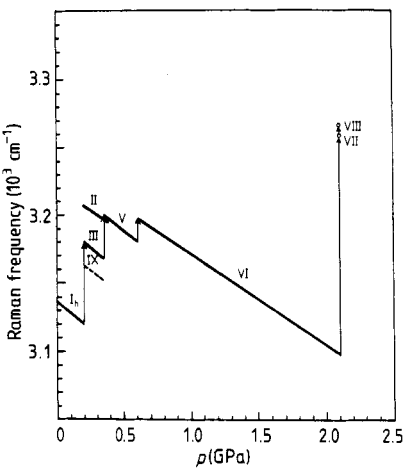

Figure 6. Schematic representation of the pressure dependences of the symmetric OH stretching vibrational bands in ice I_h, II, III, IX, V and VI of H_2O at 246 K. (The broken line shows ice IX at 150 K. The slope for ice VI is taken from Abebe and Walrafen (1979). Points for ice VII and VIII are from Wong and Whalley (1976).

the recently obtained (Abebe and Walrafen 1979) value of $\partial\nu/\partial p$ for ice VI of $-72 \pm 2\,\mathrm{cm}^{-1}$/GPa fits in well with our values. The OD stretching vibrations show corresponding shifts with temperature and pressure, in that the values of $\partial\nu/\partial p$ and $\partial\nu/\partial T$ are approximately a factor of $\sqrt{2}$ smaller than those in the H_2O ices (table 2).

The pressure-dependent behaviour of the hydrogen bond in different ice forms and the effects of the phase transitions are illustrated by figure 6. As the pressure is applied to a given ice structure, the hydrogen bond seems to strengthen, which is reflected in the decrease of the OH stretching frequency. On passing through the phase transition, a new phase appears which exhibits weaker hydrogen bonds as shown by the sudden 'jump' of the OH stretching frequency at the transition. The most dramatic changes happen when ice I_h transforms into ice III (IX) or ice II, and when ice VI transforms into ice VII (VIII).

The results can be compared with the crystallographic data. The tetrahedral angles deform from the 'ideal' angle of about 109° in ice I_h at zero pressure (Peterson and Levy 1959) into angles between 80 and 140° in ice II (Kamb *et al* 1971) or ice IX (La Placa *et al* 1973). During the ice I_h–II or I_h–III (IX) transformations, the O–O distances lengthen from 275 pm (in ice I_h) to about 280 pm (in ice II). As a result of the bending of the O...O...O angles and lengthening of the hydrogen bonds, the O–H...O (O–D...O) bonds tend to deviate from linearity, as shown by the neutron diffraction measurements on ice II (Kamb *et al* 1971) and ice IX (La Placa *et al* 1973).

The transitions from ice III to ice V and from ice V to ice VI seem to have little effect on the O...O...O angles (La Placa *et al* 1973, Kamb *et al* 1967, Kamb 1965). At the transition from ice VI to ice VII (or VIII) figure 6 shows another dramatic change. Crystallographic data on ice VIII (Kamb and Davis 1964) have shown that the nearest-neighbour hydrogen-bonded O...O distances are at 295 pm, the nearest-non-bonded neighbours are at 280 pm, while the O...O...O angles have about the 'ideal' value of about 109°.

Figure 6 shows that in the range of pressure from 0.0001 to 2.2 GPa (in which all

known ice–ice transitions occur) the frequencies of the ν_1 OH stretching modes always fall within a relatively narrow range. It is instructive to see how in each phase the hydrogen bond strengthens as pressure is applied, but weakens discontinuously as increasing pressure causes each successive phase change.

3.3. General features of the Raman spectra of the translational vibrations

The Raman spectra due to translational vibrations in the different phases of ice examined in our experiments are shown in figure 7(*a*). The last spectrum belongs to ice VIII and has been recorded (Wong and Whalley 1976) at atmospheric pressure and 100 K. In figure 7(*b*) the comparable far-infrared spectra are shown (Whalley and Bertie 1967, Bertie and Whalley 1967, Bertie 1968).

The variety of O . . . O distances and O–O–O angles in these different ices enriches the lattice vibration spectrum. However, except for ice I_h and ice I_c, there seem to be no firm assignments for the bands in this spectral region. In the last ten years detailed lattice

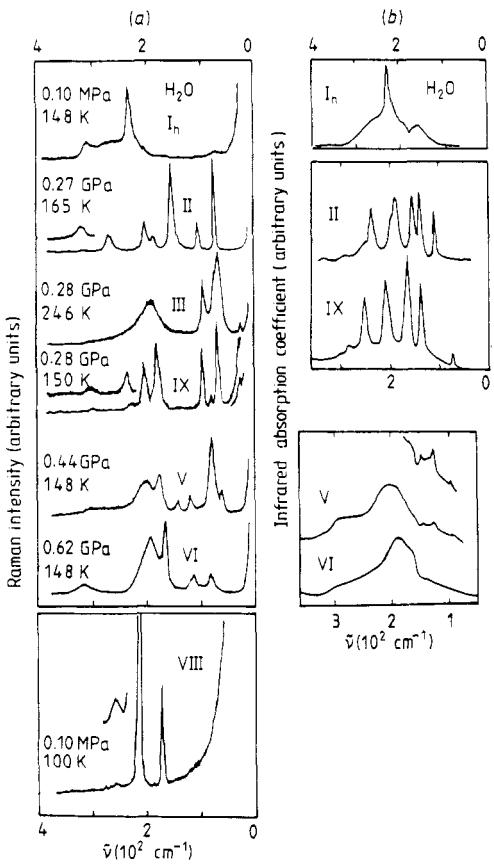

Figure 7. (*a*) The Raman spectra of the I_h, II, III, IX, V, VI and VIII forms of ice in the region of lattice vibrations at pressures and temperatures as indicated. (Res. 3–4 cm^{-1}). (Data for ice VIII are from Wong and Whalley (1976). (*b*) Far-infrared spectra of I_h, II, IX, V and VI at atmospheric pressure and 100 K (from Whalley and Berti (1967), Bertie and Whalley (1967), Bertie (1968)).

dynamical calculations on the hypothetical ordered form of ice I_h and I_c have been published (Renker 1969, Prask *et al* 1972, Shawyer and Dean 1972, Bosi *et al* 1973, Wong *et al* 1973). The infrared and Raman spectra of these ices below about 230 cm^{-1} are in general understood in terms of two force constants, the O...O stretching and the O–O–O bending force constants. Some preliminary lattice dynamical calculations on ordered ice forms (II, IX) have been made recently (Bertie and Francis 1982). The simple model used in these calculations described the observed bands quite well.

In the absence of a complete neutron determination of the phonons of the various structures, three main sources of experimental data contribute to our understanding of the lattice vibrations:

(*a*) crystallographic data published for different ice phases;
(*b*) available spectroscopic data: far-infrared and Raman spectra;
(*c*) pressure-induced shifts as measured from our Raman experiments.

(*a*) Crystallographic data on high-pressure polymorphous ices (Kamb 1969, 1973) show the variety of crystal forms that exist. Table 3 presents, in a condensed form, the available crystallographic data for all known forms of ice. Note that the number of distinct water molecules per unit cell (and therefore the number of different O...O separations) increases from ice I_h through ice II, III (IX) up to ice V, after which it starts to decrease again through ice VI and ice VII (VIII).

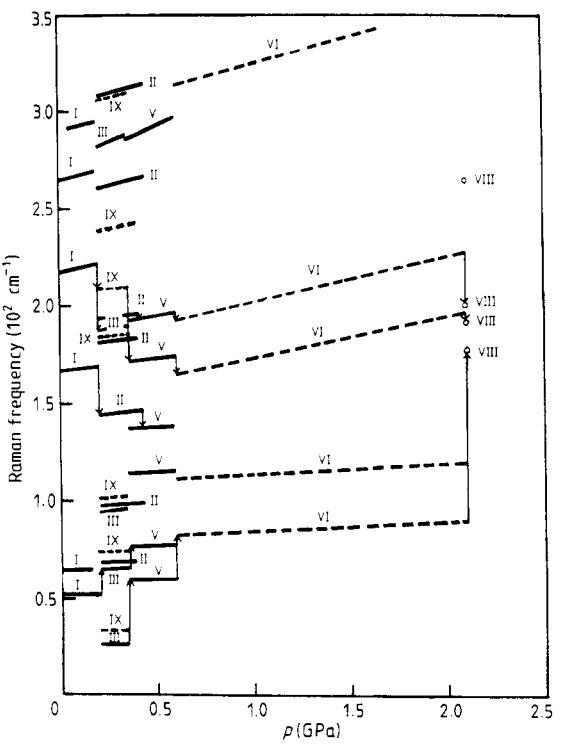

Figure 8. Schematic representation of the pressure dependence of the bands due to lattice vibration at 246 K (H_2O). (The slopes for ice VI are extrapolated on the basis of our data. The points for ice VIII are from Wong and Whalley (1976).)

(*b*) The available spectroscopic data, the Raman spectra, and the far-infrared spectra (recorded at atmospheric pressure and 100 K) are presented in figure 7. Both infrared and Raman spectra show sharper bands for the ordered structures than for the disordered structures, but this effect is more pronounced in the infrared. For the Raman spectra the most striking difference is between that of ice I_h and all other phases of ice. Except for the weak band at about 50 cm^{-1}, no other bands are observed in the spectrum of ice I_h until 220 cm^{-1}, where the strongest band appears. In contrast, all other ice forms have nearly all their Raman bands in the spectral region between these two bands.

(*c*) The rate of change of frequency with pressure has been measured for nearly all the bands due to translational vibrations in the forms of ice examined in our experiments except for ice VI. All the data are collected and presented in figure 8. The slopes of the lines $\partial\nu/\partial p$ for every band are given in tables IV.2, V.2, and VI.2 of Sukarova (1982). The accuracy of the $\partial\nu/\partial p$ values was not high, and varied depending on the ice examined. Nevertheless, figure 8 is useful for helping with the band assignments in this spectral region. Figure 8 indicates that bands below 100 cm^{-1} show an average shift of about +7 cm^{-1}/GPa which is about half that for the bands over 100 cm^{-1}. It is generally found that transverse acoustic mode frequencies are significantly less pressure sensitive than other modes. Therefore, the small pressure-induced shifts of the bands below about 100 cm^{-1} might be taken to imply that they have some transverse–acoustic-like character. Figure 8 shows also that the frequencies of these bands increase at the phase transitions in going from less dense to more dense forms of ice, which is again the behaviour expected for this type of mode.

On the other hand, the bands above about 100 cm^{-1} but below about 220 cm^{-1} show values $\partial\nu/\partial p$ which are significantly more pressure sensitive. They rise in frequency quite rapidly within any one phase and at the phase transitions the frequencies drop in going to the denser phases. This kind of behaviour is expected for the optic modes as well as for the longitudinal acoustic modes. For example the TO modes of the alkali halides show this effect in the NaCl-type to CaCl-type transformations (Lowndes and Rastogi 1976, Sherman 1982).

A transformation from ice I_h to ice II, or ice I_h to ice III (IX) allows more efficient packing. Thus although the transition is accompanied by a marked *decrease* in volume, there is a marked *increase* in the O–H...O (O–D...O) distances; this is indicated by the drop in the optic-mode frequency at the phase transition. The steady increase of the optic mode frequency with pressure within any one phase indicates the steady decrease in the O–H...O (O–D...O) distances as that phase is compressed.

The crystallographic data (table 3) and the far-infrared and Raman spectra (figure 7) and pressure-induced shifts as measured in our experiments (figure 8) form a valuable data set for the re-evaluation of the lattice vibrational properties of these forms of ice. For a detailed analysis, a theoretical study of the dispersion curves of different ice phases is needed, which is beyond the scope of this present paper. However some general observations are made below and the detailed results of our calculations will be given elsewhere.

In the large unit cells of the various ice forms, the number of branches in the dispersion curves becomes such that one would expect a rather crowded diagram in the 0–350 cm^{-1} region where the translational vibrations of the water molecules are expected. However, the relatively simple Raman (and far-infrared) spectra of ice of types II, III (IX), V, VI and in particular ice VIII suggest that there should be an approximate explanation of these bands in terms of the higher symmetry and/or the smaller unit cells to which the structures approximate. The fact that Bertie and Francis

Table 3. Collected crystallographic data for all known ice phases.

Ice	Crystal system	Point group	Z[a]	Density ($Mg\ m^{-3}$)	Number of distinct water molecules	Number of O . . . O separation	$R_{(O\ldots O)}$ (pm)
I_h	$P6_3/mmc$[b]	D_{6h}	4	0.931	1	1	275
I_h	$P6_3mc$[c]	C_{6v}	4	—	—	—	—
I_h	Pmc_1[c]	C_{2v}	4	—	—	—	
I_c	$Fd3m$[d]	O_h	8	0.93	1	1	275
I_c	$I4_1md$[c]	C_{4v}	2	—	—	—	—
II	$R\bar{3}c$[e]	D_{3f}	12	—	—	—	284.4 280.3
II	$R\bar{3}$[f]	$C_{3i}=S_6$	12	1.18	2	4	278.1 276.8
III	$P4_12_12$[e]	D_4	12	(1.16)	—	—	275.0 276.3
IX	$P4_12_12$[g]	D_4	12	1.16	2	3	279.3
IV	$R\bar{3}c$[h]	D_{3d}	16	1.27	2	4	290 288 282 279
V	$A2/a$[i]	C_{2h}	28	1.23	4	8	286.7 282.0 281.9
V	Aa[c]	C_S					279.8 278.2 278.1 276.6 276.6
VI	$P4_2/nmc$[j]	D_{4h}	10	1.31	2	3	279
VI	$Pmmn$[j]	D_{2h}	—	—	—	—	281
VI	Pm[c]	C_S	—	—	—	—	282
VIII	$Pn3m$[k]	O_h	2	(1.49)	1	1	295
VIII	$I4_1/amd$[l]	D_{4h}	8	1.49	1	1	295

[a] Number of molecules per unit cell
[b] Hypothetical, fully disordered structure. Hydrogens midway between the oxygen atoms.
[c] Hypothetical fully ordered structure.
[d] Fully disordered, hydrogens half way between the oxygen atoms.
[e] Hypothetical partial disorder.
[f] Ordered structure.
[g] Nearly complete order (~4% partial disorder).
[h] Most probably partial disorder.
[i] Partial disorder.
[j] Hypothetical fully disordered structure.
[k] Full disorder.
[l] Full order.

(1982) were able to reproduce the far-infrared and Raman spectra of the ordered forms of ice II and ice IX with a relatively simple force field model also indicates that a general assignment of these bands could be relatively simple. It seems that the best starting points for a simple consideration of the dispersion curves of the different ice phases is the data on ice VIII and ice I.

Both ice VIII and ice I have H--O--H and O---O---O angles which are close to the 'ideal' value of 109°. Thus both structures approximate to simple tetrahedrally bonded systems with linear hydrogen bonds. It is the proton positions alone which stop these structures from being effectively 'diamond-like' for ice I_c† and 'two interpenetrating diamond-like structures' for ice VIII.

However, the *frequencies* of the translational lattice modes are unlikely to be significantly affected by the proton positions.

The infrared and Raman activities of the modes may well be affected by the proton positions, but the frequencies are determined by the relevant masses and force constants and these are *not affected* by the proton positions. Note that the isotopic shifts ($H \rightarrow D$ and $^{16}O \rightarrow {}^{18}O$) show (i) that there is no more than possibly a very slight mixing of rotational and translational lattice modes, and (ii) that there is no detectable mixing of lattice modes with O–H stretching or bending vibrations. This explains why the translational modes can be described quite realistically by simplified models in which tetrahedrally bonded masses of mass 18 amu (H_2O) or 20 amu (D_2O) vibrate against one another.

The basic model for the translational vibrations of ice I is therefore that of a diamond-like structure and for ice VIII it is a structure formed by the interpenetration of two diamond-type lattices. Some of the translational modes of the various ice structures show quite large infrared intensities and even the basic model should show this. For example, a rigid-ion model would need to include an effective charge separation between the non-equivalent water molecules. This would supply the (otherwise missing) dipole moment during the vibrations and would also result in LO → TO splittings for the infrared-active modes (cf zincblende structure).

In relating the vibrational properties of such models to the observed infrared and Raman spectra there are two essentially independent problems. (i) The calculation of the vibrational properties of the model, which will be completely independent of the positions of the protons. (ii) The determination of the infrared and Raman activities of the various vibrations, which will depend very markedly on the proton positions. For example, the oxygen positions of an idealised ice VIII structure form a body centred cubic lattice which would have no first-order infrared or Raman spectra of any kind. However the protons: (i) reduce the oxygen site symmetry from O_h to C_{2v}, (ii) introduce a dipole moment at each oxygen (H_2O) site, (iii) cause physical distortion of the idealised cubic lattice (making it necessary to define a larger unit cell) and (iv) cause several of the vibrations to gain infrared or Raman activity, without (it is hoped) dramatically altering their forms or frequencies.

It is therefore proposed that models of simple diamond-like (more strictly zincblende-like) structures could be expected to predict fairly accurately the translational modes of vibration of the various ice lattices. An indication of the infrared and Raman activities that might be expected for the different modes of these models should be predictable by the technique of 'folding of the dispersion curves' of the simple model

† Note that ice I_c and ice I_h have similar spectra and therefore calculations for I_c can be assumed to apply also to I_h.

to achieve the appropriate cell size (and symmetry) of the real lattice. Most of the frequencies should require little more than a general scaling by the factor $\sqrt{k}$, where k is the stretching force constant of an (H_2O)–(H_2O) bond. (This will not be true for those modes originating from the TA modes of the basic model and it is likely to be a poor approximation for any modes which rely heavily on restoring forces which originate from bond bending. However the assumption is useful in producing a very simple model, and partially justified by the small overall change in k.)

One point that must be made very clearly, is that neither the infrared nor the Raman spectra of the proton-disordered forms can be expected to show 'density-of-states'-type spectra.

Short-range order is imposed by the restriction that one proton only is allowed on any one O---O bond. This is enough to ensure that the spectra are overwhelmingly dominated by features which are allowed by the selection rules of the (hypothetical) ordered form.

For example the ice III and ice IX Raman spectra are very similar to one another and quite different from the infrared spectra. The proton disorder in ice III has broadened the spectra by introducing a range of different (but at short range very similar) proton arrangements within the crystal. It has *not* given any significant activity to any of the modes which the ordered ice IX structure rendered inactive.

We see this as a clear and important example of the limited spectroscopic effects introduced by rotational disorder within translationally ordered crystals.

Thus the ice $I_c(I_h)$ spectra would be expected to be zincblende like. The infrared spectrum should be dominated by the TO_Γ mode of the basic (two atoms/unit cell) zincblende structure and the Raman spectrum should be dominated by the TO_Γ and LO_Γ of that model.

Minor differences might be looked for between the spectra of ices I_c and I_h. These would be expected to arise mainly from the different symmetry and changes in cell size required by the different hypothetically full proton-ordered structures of ices I_c and I_h.

'Ordered I_c' would be a C_{4v} structure with 2 molecules/unit cell (Kamb 1969, 1973). The zincblende (T_d) model has 2 molecules/unit cell, an F_2 acoustic mode (splitting into LA and TA away from the zone centre) and an F_2 optic mode (which is split into LO and TO even at the zone centre). However, C_{4v} is not a subgroup of T_d and in order to establish the correlation between the model and the activities to be expected under C_{4v} rules it is easiest to set the charge separation in the model to zero (making it O_h) and correlate $O_h \rightarrow C_{4v}$.

For an O_h model (2 molecules/unit cell, diamond like) the acoustic mode is F_{1u} and the optic mode is F_{2g} (see table 4).

A consideration of the forms of the displacements make it clear that the splittings ($F \rightarrow B_2$ (or A_1) + E) are equivalent to the LA + TA and LO + TO splittings in the zinc-

Table 4.

Model ($z = 2$)	Ic ($z = 2$)		1h ($z = 4$)
O_h	C_{4v}		C_{2v}
F_{2g}	B_2 — R_{XY}	$\rightarrow$	$2A_2$ (or A_1) − (IR) R_{XY}
	E IR $R_{XZ,YZ}$	$\rightarrow$	2 ($B_1 + B_2$) IR $R_{XZ}R_{YZ}$
F_{1u}	A_1 IR $R_{XX,YY,ZZ}$	$\rightarrow$	$2A_1$ IR $R_{XX,YY,ZZ}$
	E IR $R_{XZ,YZ}$	$\rightarrow$	$2(B_1 + B_2)$ IR R_{XZ} R_{YZ}

blende model. The C_{4v} (2 molecules/unit cell) selection rules show that for ice I_c that no extra features are expected beyond those predicted by the simple T_d model.

Ordered ice I_h has 4 molecules/unit cell and can have C_{6v} or C_{2v} symmetry depending on the details of the ordering (Kamb 1969, 1973). Using the above cell geometries, the equivalent reciprocal lattices can be constructed and superimposed on that of the zincblende model. This allows the splitting shown by the correlation table to be interpreted in terms of a 'folding of the Brillouin zone' of the basic model. It is possible to obtain some information in this way even when the larger unit cell has a symmetry that is not a subgroup of that of the high-symmetry model. For example, the C_6 axis of the C_{6v} symmetry ice I_h can be associated with a cube diagonal of the O_h model. Then in reciprocal space the hexagonal net of the ice I_h has a hexagonal prism Brillouin cell which closely overlaps the truncated octahedral cell of the BCC net of O_h except along the C_6 axis. Along the C_6 axis the hexagonal net repeats twice as frequently as the O_h net and puts a C_6 Γ point onto an O_h L point. This suggests that the dispersion curves of the O_h model should be 'folded' so as to bring the L point into the zone centre in order to predict the C_{6v} spectrum. Thus TA_L becomes an E-type Γ mode (B_1 and B_2 split in the C_{2v} form), LA_L becomes an A_1 mode, TO_L gives a further E mode (B_1 and B_2 split in C_{2v}) and LO_L gives an A_1 mode (A_2 or A_1 in C_{2v} depending on whether σ_v or σ_d is retained).

It has proved possible to extend this type of argument to include some of the other ice forms. However a full description of that work together with the details of the models used in the calculations, makes a long paper by itself. That work is therefore being

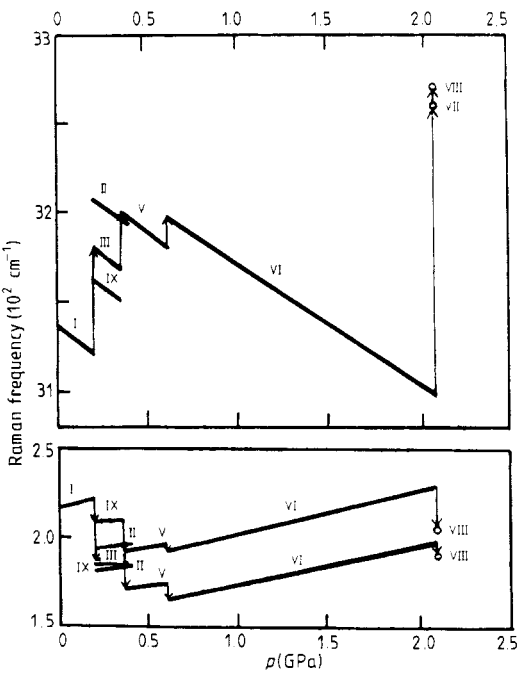

Figure 9. The effect of pressure on the O–H stretching frequency and the 'diamond-like' lattice mode frequency for various ice structures. Note that within a given structure pressure decreases the O...O distances and increases the O–H distances as shown by increasing lattice mode frequencies and decreasing O–H stretching frequencies. Phase transitions have the opposite effect.

prepared for publication elsewhere. It should nevertheless be clear from the above introduction to that work (and a consideration of figures 7, 8 and 9) that the general form of these spectra and their pressure dependences can all be understood in terms of modifications of a single simple model.

4. Conclusions

Experiments have been described in which good quality Raman spectra of the I, II, III, IX, V and VI forms of ice have been studied as functions of temperature and pressure within their regions of true thermodynamic stability. The wealth of data collected in this series of experiments could not possibly be analysed within a single paper (although most of it has been considered within a 380 page thesis, Sukarova 1982). However the preliminary discussion given here indicates the significance of this work, makes available the basic results, and creates a background against which the detailed analyses of specific aspects of the work can be set.

Acknowledgments

The financial support given by the SERC and the US Army in support of our high-pressure spectroscopic laboratory is gratefully acknowledged, as is the gift of the $H_2{}^{18}O$ by Dr Straschewski of the Institut fur Neutronen Physik, Karlsruhe.

References

Abebe M and Walrafen G E 1979 *J. Chem. Phys.* **71** 4167
Bertie J E 1968 *Appl. Spectrosc.* **22** 634
Bertie J E and Bates F E 1977 *J. Chem. Phys.* **67** 1511
Bertie J E and Francis B F 1980 *J. Chem. Phys.* **72** 2213
—— 1982 *J. Chem. Phys.* **77** 1
Bertie J E, Labbe H J and Whalley E 1968 *J. Chem. Phys.* **49** 2141
Bertie J E and Whalley E 1964 *J. Chem. Phys.* **40** 1646
—— 1967 *J. Chem. Phys.* **46** 1271
Bosi P, Tubino R and Zerbi G 1973 *J. Chem. Phys.* **59** 4578
Bridgman P W 1912 *Proc. Am. Acad. Arts. Sci.* **47** 441
—— 1935 *J. Chem. Phys.* **3** 597
—— 1937 *J. Chem. Phys.* **5** 964
Hawke R S, Syassen R and Holzapfel W B 1974 *Rev. Sci. Instrum.* **45** 1593
Hirsh K R and Holzapfel W B 1980 *Rev. Sci. Instrum.* **52** 52
Holzapfel W B, Hawke R S and Syassen K 1974 *Proc. IVth Int. Conf. on High Pressure (Kyoto)* p 344
Johari G P and Sivakumar T C 1978 *J. Chem. Phys.* **69** 557
Kamb B 1965 *Science* **150** 205
—— 1969 *Trans. Am. Cryst. Assoc.* **5** 61
—— 1973 *Physics and Chemistry of Ice* ed. E Whalley, S J Jones and L W Gold (Ottawa: Royal Society of Canada) p 28
Kamb B and Davis B L 1964 *Proc. Natl Acad. Sci. USA* **52** 1433
Kamb B, Hamilton W C, La Placa S J and Prakash A 1971 *J. Chem. Phys.* **55** 1934
Kamb B, Prakash A and Knobler C 1967 *Acta Crystallogr* **22** 706
Kennedy J, Sherman W F, Treloar N and Wilkinson G R 1976 *Proc. 5th Int. Conf. on Raman Spectroscopy (Freiburg) 1976* (Freiburg: Schulz)
La Placa S J, Hamilton W C, Kamb B and Prakash A 1973 *J. Chem. Phys.* **58** 567

Lavergne A and Whalley E 1979 *Rev. Sci. Instrum.* **50** 962
Lowndes R P and Rastogi A 1976 *Phys. Rev.* B **14** 3598
Noack R A and Holzapfel W B 1977 *Proc. 6th AIRAPT, Int. Conf. on High Pressure (Boulder, Colorado) 1977*
Peterson S W and Levy H A 1959 *Acta Cryst.* **10** 70
Piermarini G J, Block S, Barnett J D and Forman R A 1975 *J. Appl. Phys.* **46** 2774
Prask H J, Trevino S F, Gault J D and Logan K W 1972 *J. Chem. Phys.* **56** 3217
Renker B 1969 *Phys. Lett.* **30A** 493
Shawyer R E and Dean P 1972 *J. Phys. C: Solid State Phys.* **5** 1028
Sherman W F 1982 *Bull. Soc. Chim. de France* **9** 347
Sherman W F and Wilkinson G R 1980 *Advances in Infrared and Raman Spectroscopy* vol 6, ed. R J Clark and R E Hester (London: Heydon) ch IV, p 158
Sivakumar T C, Chew H A M and Johari G P 1978 *Nature* **275** 524
Sukarova B 1982 *PhD Thesis* King's College, London
Sukarova B, Sherman W F and Wilkinson G R 1982 *J. Mol. Struct.* **79** 289
Tammann G 1900 *Ann. Phys., Lpz* **21** 1
Walrafen G E 1973 *J. Solut. Chem.* **2** 159
Whalley E 1975 *J. Chem. Phys.* **63** 5205
—— 1977 *Can, J. Chem.* **55** 3429
Whalley E and Bertie J E 1967 *J. Chem. Phys.* **46** 1263
Whalley E, Heath J B R and Davidson D 1968 *J. Chem. Phys.* **48** 2362
Whalley E and Lavergne A 1976 *Rev. Sci. Instrum.* **47** 136
Wong P T T, Klug D D and Whalley E 1973 *Physics and Chemistry of Ice* ed. E Whalley, S J Jones and L W Gold (Ottawa: Royal Society of Canada) p 278
Wong P T T and Whalley E 1976 *J. Chem. Phys.* **64** 2359